

“Radiological Evaluation of Spectrum of Neurooncological Pathologies: Our Experience in a Tertiary Care Hospital of Eastern India”

Dr. Nupur Basu¹, Dr. Prithvijit Chakraborty^{2*}

¹Assistant Professor, Medical College & Hospital, Kolkata

²Resident, Medical College & Hospital, Kolkata

*Corresponding Author: Dr. Prithvijit Chakraborty

Abstract:-

Objectives- The clinical presentations of brain and spinal cord tumors are often non-specific. Their prognosis mostly depends on early and timely correct diagnosis. Radiological imaging is probably the only diagnostic method with good sensitivity and specificity for critical detection and diagnosis. In this study we have studied the spectrum of imaging findings of malignant brain and spinal cord tumors presented in our institute and retrospectively evaluated the imaging features that may help in early diagnosis and treatment of those conditions and improve the quality of life.

Methods:- We analysed the imaging features of 56 patients with neoplastic pathologies of brain and spinal cord between September 2018 and February 2019 after they met the inclusion criteria. Imaging findings of each patients were studied, analysed and classified based on the spectrum of neoplastic brain and spinal cord pathologies.

Results:- Average age of male adult patients was 67 years and that of female adult patients was 55 years. Average age of male pediatric patients was 6 years and that of female pediatric patients was 7.1 years. Most common brain tumor in adults were metastasis. Most common primary for brain metastasis was from lung carcinoma. Among the primary brain tumors among adult patients, most were anaplastic astrocytoma (Grade III). Among the primary brain tumors in pediatric patients, most (33.3%) were medulloblastoma.

Conclusion:- Imaging evaluation with magnetic resonance imaging (MRI) plays an important role in diagnosis and timely management of brain and spinal cord tumors.

Keywords:- Neurooncology; Brain Tumor; Spinal cord tumor; Astrocytoma; Medulloblastoma; Glioblastoma multiforme; Magnetic Resonance Imaging;

Date of Submission: 15-04-2019

Date of acceptance: 30-04-2019

LIST OF ABBREVIATIONS:-

MRI= Magnetic Resonance Imaging;
BOLD= Blood Oxygen Level-Dependent;
DWI= Diffusion-Weighted Imaging;
DSC= Dynamic Susceptibility Contrast;
DCE= Dynamic Contrast-Enhanced;
ASL= Arterial Spin Labeling;
NAA= N-acetyl aspartate;
rs-fMRI= resting state functional MRI;
FLAIR= Fluid-Attenuated Inversion Recovery;
DMN= Default Mode Network;
rCBV= Relative Cerebral Blood Volume;

I. Introduction

The clinical presentations of brain and spinal cord tumors are often non-specific. Their prognosis mostly depend on early and timely correct diagnosis. Radiological imaging is probably the only diagnostic method with good sensitivity and specificity for critical detection and diagnosis. With the availability of MRI, perfusion imaging, diffusion-weighted imaging, MR spectroscopy, blood oxygen level-dependent (BOLD) imaging, the diagnostic yield has improved significantly. In recent years, a great deal has been learned about the molecular and genetic origins of brain tumors, and in 2016 WHO updated its primary brain tumor classification schema to directly incorporate genetic information for the first time. In this study we have studied the spectrum

of imaging findings of malignant brain and spinal cord tumors presented in our institute and retrospectively evaluated the imaging features that may help in early diagnosis and treatment of those conditions and improve the quality of life.

II. Materials And Methods

A retrospective study was done at our institute between September 2018 to February 2019. 56 patients of brain and spinal cord tumors referred to our department for review of their imaging features were included in the study after they met the inclusion criteria.

Institutional Ethics Committee: Approval from institutional ethics committee obtained.

Inclusion criteria:

1. Patients of neoplastic brain and spinal cord pathologies detected clinically, Radiologically or Histopathologically.
2. Patients having brain and spinal cord metastasis were included in the study.
3. Patients who gave consent to take part in the study.

Exclusion criteria:

1. Patients having non neoplastic brain or spinal cord space occupying lesions.
2. Patients having neoplastic lesion of central nervous system outside the cranium and spinal canal and tumors of peripheral nervous system.
3. Patients who refused to take part in the study.

Procedure:

Before the data of the patients were collected and analysed, following informations were obtained-

- Age, Sex
- History of present illness, past history, drug history and family history of neoplastic disorders
- Clinical features and examination findings were noted
- Records of baseline laboratory investigations like Complete Blood Count, serum lipid profile, blood sugar, serum creatinine, ECG, Chest X-ray were noted.
- Radiologic imaging features (Contrast Enhanced Computed Tomography, Conventional MRI T1W,T2W, T2-FLAIR, GRE, SWI, DWI & ADC and MRS) were reviewed and recorded.
- Histopathologic features were also noted.

Findings were recorded in predesigned and pretested case record sheet for subsequent analysis.

III. Results

Among 56 patients (M= 31, F= 25; Average age= 61.6 years), 42 patients were adults and had Brain tumors (M= 25,F=17). Among those 42 patients, 29 patients had primary brain tumors, rest of 14 had metastatic tumors in brain. Majority (42.8%) of metastasis were from Lung carcinoma, where other source of primaries were Breast carcinoma (28.6%), Renal Cell Carcinoma, Colon carcinoma, Chorio-carcinoma and Thyroid Carcinoma (each 7.1%). 12 patients were from pediatric age group (M= 4, F= 8). 2 patients had spinal cord tumors (both male) , one of them had spinal neurofibroma. Another patient had spinal drop metastasis from his primary glioblastoma multiforme. Average age of the patients with spinal cord tumors was 56.9 years. The average age of pediatric patients was 6.7 years. Average age of male pediatric patients was 6 years and that of female pediatric patients was 7.1 years. Average age of male adult patients was 67 years and that of female adult patients was 55 years. Among the primary brain tumors among adult patients, 41.3% were astrocytoma, 31% were meningioma, 13.8% were pituitary adenoma, 10.3% were schwannoma, 3.4% were pineoblastoma. Among the astrocytoma in adults, 41.6% were Anaplastic (Grade-III), 33.3% were diffuse (Grade-II), 16.7% were Glioblastoma Multiforme (Grade- IV) and 8.3% were pilocytic astrocytoma (Grade-I). Among the Pituitary tumors, all were macroadenoma. Of them, 50% were non functioning type, 25% were predominantly prolactinoma and 25% were mixed prolactin/GH secreting tumor. Among the primary brain tumors in pediatric patients, 33.3% were medulloblastoma, 25% were astrocytoma, craniopharyngioma and teratoma were 16.8% each and 8.1% were atypical rhabdoid/teratoid tumor. All the astrocytoma of pediatric age group were of pilocytic (Grade-I) type.

IV. Discussion

In spite of the rapid progress of magnetic resonance imaging, conventional structural magnetic resonance imaging (MRI) remains the standard of care imaging method for neurooncologic practice. Current consensus recommendations for a standardized brain tumor MRI protocol are the following: 3-dimensional (3-D) T1, axial fluid-attenuated inversion recovery (FLAIR), axial diffusion-weighted imaging (DWI), axial

gadolinium contrast-enhanced T2, and 3-D gadolinium contrast-enhanced T1, performed on a minimum 1.5 tesla MR system. If 3-D sequences cannot be performed due to time constraints or technical limitations, 2-D sequences can be substituted. The structural sequences (T2-weighted, FLAIR, and pre- and postcontrast T1-weighted) provide the primary foundation of an MRI examination. Specific presurgical sequences such as high-resolution isovolumetric 3-D T2-weighted and postcontrast 3-D T1 spoiled gradient recalled echo imaging can be obtained with fiducial markers for intraoperative navigation or with a head frame for stereotactic radiosurgical planning. In addition to conventional structural sequences, DWI and T2*-weighted imaging, such as susceptibility-weighted imaging (SWI), are usually performed as part of the routine brain MRI examination.^[1] MRI offers superior soft tissue contrast over other cross-sectional imaging techniques allowing for better visualization of subtly infiltrated or disrupted parenchymal architecture. Furthermore, intravenous gadolinium-based contrast agents shorten T1 relaxation times and increase tissue contrast by accentuating areas where contrast agents have leaked out of the blood–brain barrier (BBB) into the interstitial tissues, resulting in parenchymal enhancement. This breakdown of the BBB is a key feature seen in tumors as well as non-neoplastic conditions. The region of T2/FLAIR hyperintense signal abnormality surrounding the enhancing tumor core is typically referred to as peritumoral edema and can be vasogenic or infiltrative in nature. Vasogenic edema represents a reactive increase in extracellular water due to leakage of plasma fluid from altered tumor capillaries in the absence of tumor cells and is seen around intracranial metastases or noninfiltrative extra-axial tumors such as meningiomas. Infiltrative edema in gliomas represents a mixture of vasogenic edema and infiltrating tumor cells invading along, but not necessarily disrupting, white matter tracts and can be considered nonenhancing tumor owing to preserved integrity of the BBB.^[2]

Primary lesion location can help differentiate between tumor types. For example, extra-axial tumors such as meningiomas, schwannomas, and skull base tumors can generally, but not always, be differentiated from intra-axial tumors based on associated interposition of cerebrospinal fluid, vessels, or dura between the mass and cortex. Similarly, the number of lesions is an important consideration as multiple lesions suggest metastatic disease or non-neoplastic processes such as demyelination, inflammation, or infection. Finally, several imaging characteristics suggest tumor subtypes. The combination of a cyst and solid nodule within a tumor suggests brain tumors such as ganglioglioma, pilocytic astrocytoma, pleomorphic xanthoastrocytoma, and, in the posterior fossa, hemangioblastoma. Calcifications can be seen in oligodendrogliomas, ependymomas, and pineal tumors, among others. Necrosis and hemorrhage are seen with higher grade gliomas, certain metastases, and rarely central nervous system (CNS) lymphoma in immunocompromised patients.^[3]

Brain tumors have been classified based on histology according to the WHO criteria. Diffuse gliomas are further subdivided into 4 grades by various histological features such as cellularity, nuclear atypia, mitotic activity, pleomorphism, vascular hyperplasia, and necrosis. Grade I gliomas including pilocytic astrocytoma, pleomorphic xanthoastrocytoma, and subependymal giant cell astrocytoma share a relatively benign biology with an indolent clinical course that is distinct from other diffuse infiltrating glioma grades. Grade II-IV gliomas are heterogeneous tumors with variable degrees of infiltration, atypia, and mitotic activity. Microvascular proliferation with endothelial hyperplasia and pseudopallisading necrosis are the defining histological hallmarks of grade IV gliomas, frequently referred to as glioblastomas. Recent insights into tumor biology have led to the identification of several molecular aberrations associated with genetic phenotypic differences in brain tumors. The updated WHO classification incorporates molecular markers along with histology and defines specific entities on the basis of IDH mutation and 1p19q chromosomal deletion. These, along with other molecular markers including p53, RB1, EGFR, PTEN, MGMT, BRAF, ATRX, TERT, and histone H3, represent a nosological shift where histopathological phenotype is complemented by molecular genetic phenotype to better classify brain tumors and predict their clinical behaviour.^[4]

DWI best serves to characterize tumor cellularity on the premise that water diffusivity within the extracellular compartment is inversely correlated to the volume of the intracellular space. Low ADC values, representing decreased water diffusivity, can be used to suggest highly cellular tumors such as lymphoma, medulloblastoma, or primitive neuroectodermal tumor (PNET). Additionally, low ADC values can be used as a surrogate for increasing tumor grade or as an independent biomarker signifying poor outcomes both in glioma and lymphoma. ADC values have also been used to better localize tumor infiltrated foci among regions of vasogenic edema to better direct tissue sampling and therapy. Because of the heterogeneous nature of intracranial tumors, particularly gliomas, histogram analysis can be employed to better assess ADC metrics.^[5]

High-resolution 3-D T2* gradient echo sequences such as SWI are highly sensitive to magnetic susceptibility effects from blood products or mineralization. This technique is useful to depict internal vascular architecture and hemorrhage in tumors, which can be used to suggest grade, as well as calcification, which can be used to narrow the differential diagnosis. Both blood products and mineralization appear dark on magnitude images and can be differentiated on filtered phase images in which paramagnetic blood products appear dark and diamagnetic calcium appears bright.^[6]

Several MR perfusion techniques are currently employed: dynamic susceptibility contrast (DSC), dynamic contrast-enhanced (DCE), and arterial spin labeling (ASL). Of these, DSC perfusion is the most studied and widely applied, while ASL, which does not require intravenous contrast, has been the subject of increasing investigation and clinical implementation. DSC is based on the detection of susceptibility induced signal loss on T2*-weighted sequences after the administration of an intravenous gadolinium contrast agent. A signal intensity time curve is generated from which relative cerebral blood volume (rCBV) and other perfusion metrics are derived. rCBV is elevated in tumor, where it is seen as a marker of angiogenesis, and has been shown to distinguish tumor from non-neoplastic etiologies with lower rCBV such as demyelinating lesions. A signal intensity time curve that does not return to baseline is seen with leaky capillaries and can suggest metastasis, meningioma, or choroid plexus tumor. rCBV has been positively correlated to glioma grade, although some lower grade gliomas such as oligodendrogliomas may have elevated rCBV.^[7]

The underlying principle behind DCE is that disordered tumor vasculature permits intravascular contrast diffusion into the interstitial compartment which is then quantifiable over a dynamic MR acquisition. The volume transfer constant or k^{trans} , a measure of capillary permeability, is the primary metric derived from DCE perfusion, can be used to grade tumors, particularly gliomas, as gliomas with increased capillary permeability are more likely to be higher grade than lower grade. Another metric quantified by DCE is v_e , an estimate of fractional extracellular extravascular space, which has been shown to be related to tumor cellularity, though a strong relationship has not clearly been established.^[8]

ASL is a noninvasive perfusion imaging technique which quantitatively measures cerebral blood flow. It uses an inversion pulse to label inflowing blood proximal to the area of imaging with subsequent subtraction of these labeled spins from control static images. ASL is of particular clinical interest due to its noncontrast technique, relative speed, ability to image the whole brain, and minimal postprocessing. Several studies have shown a promising role for ASL in quantitative characterization of tumor vascularity in meningioma, metastasis, and high-grade glioma as well as in its ability to differentiate high- from low-grade gliomas based on a degree of microvascular proliferation.^[9]

MRS provides insight into the biochemical profile of interrogated brain tissue. Proton (¹H) MRS is the most studied technique and can be performed with long (288 or 144 ms) and short (35 ms) echo times. MRS can be obtained using a single-voxel technique to a targeted region of interest or a multivoxel technique to cover a broader area and better evaluate regional biochemical differences. The most recognizable metabolite peaks on long echo H MRS include *N*-acetylaspartate (NAA) at 2.0 parts per million (ppm), creatine (Cr) at 3.0 ppm, choline (Cho) at 3.2 ppm, and myo-inositol (MI) at 3.5 ppm. NAA is a marker of neuronal viability, Cr reflects normal cellular metabolism, Cho is a marker of cell membrane turnover, and MI reflects astrocyte integrity. Lipid and lactate, which have a broad peak at 1.3 ppm, are not seen in normal tissue and considered markers of necrosis and hypoxia, respectively. A normal spectrum demonstrates upward sloping of peaks from myo-inositol to choline, forming the so-called Hunter's angle of approximately 45°. Brain tumor spectra reflect cellular turnover and loss of normal neuronal metabolites, typically as elevated Cho and decreased NAA resulting in a downward sloping appearance of metabolite peaks or reversal of the usual Hunter's angle. Generally, absolute heights of metabolite peaks are not used, and rather the peaks are analyzed as ratios such as Cho/NAA and Cho/Cr. MRS has been shown to differentiate gliomas by grade on the basis of a positive correlation between Cho/NAA and Cho/Cr ratios and grade. Additionally, lower grade gliomas have been associated with elevated MI/Cr ratio. Within regions of nonenhancing signal abnormality, elevated Cho/NAA and Cho/Cr ratios have been observed in infiltrative edema compared to vasogenic edema reflecting the increased cellularity underlying the signal abnormality.^[10]

An advanced application of diffusion imaging is DTI, which interrogates the 3-D shape of diffusion using both diffusivity (eigenvalues) and direction (eigenvectors). The principle metrics obtained from

DTI include mean diffusivity (MD) and fractional anisotropy (FA). In presurgical planning, DTI-based tractography is used to guide surgical resection by analyzing the integrity of white matter fiber trajectory in order to determine whether there is tumor invasion or tumor displacement of the adjacent white matter tracts. FA represents the degree of directionality of water diffusion and in the normal brain reflects the presence of intact myelinated white matter tracts. In brain tumors, disrupted cellular architecture results in altered FA that correlates to cellularity. The identification and preservation of white matter tracts is also important in preserving the neurological functional integrity of patients undergoing resection of lesions near eloquent cortex.^[11]

fMRI indirectly measures neuronal activity using the ratio of deoxyhemoglobin to oxyhemoglobin as a contrast mechanism, known as blood oxygen level dependent (BOLD) signal. In task-based fMRI, the patient alternates between a passive resting state and task performance, usually motor or language function, while relative changes in BOLD signal are measured and used to infer areas of cortical activation. Anatomic areas localized with task-based fMRI have been validated to approximate functional sites identified with cortical stimulation mapping. Apart from localizing eloquent cortex, task-based fMRI can be used to characterize tumors. Decreased BOLD signal is noted in cortex involved by tumor and differences are also seen between

high- and low-grade tumor suggesting alterations in cerebral blood volume of the tumor affected area. fMRI can also be applied to guide DTI by delineating a seed region for fiber tractography. Recently, there has been increased interest in resting state functional MRI (rs-fMRI), which does not require patient cooperation with task paradigms and can be performed under anesthesia. rs-fMRI detects spontaneous low-frequency fluctuations in the BOLD signal between regions that are spatially distinct to identify functional networks, so-called resting state networks (RSNs). The most fundamental RSN is the default mode network (DMN) and evidence regarding other RSNs including somatosensory, visual, auditory, language, attention, and cognitive control networks is evolving.^[12]

Brain tumor follow-up imaging reflects both treatment effect and natural evolution of tumor. Typically, increasing contrast enhancement and increasing nonenhancing signal abnormality represent progressive disease. Pseudoprogession, an inflammatory response marked by a transient increase in contrast enhancement and edema upon completion of chemoradiotherapy, is observed in up to 30% of high-grade glioma patients and can also be seen in the setting of low-grade glioma.^[13] The hallmark of pseudoprogession is subsequent stabilization or improvement of contrast enhancement at follow-up MRI. The updated Response Assessment in Neuro-Oncology (RANO) criteria stipulate that within the first 12 wk following completion of radiotherapy, progression can only be determined if new enhancement is seen outside of the radiation field or if there is histopathological confirmation of tumor growth. Pseudoresponse represents a marked decrease in contrast enhancement on MRI related to diminished leakiness of the BBB following treatment with antiangiogenic agents, most commonly bevacizumab, in patients with recurrent glioblastoma. The marked decrease in contrast enhancement, and often in peritumoral edema, can be observed as early as 1 day after initiation of antiangiogenic therapy and does not necessarily reflect biological antitumor effect of therapy.^[14] In addition to mimics of tumor progression, several other chronic changes attributable to brain tumor therapy are well cataloged. Symmetric white matter signal abnormality representing gradual demyelination, gliosis, and vascular injury following chemotherapy, radiotherapy, or both is associated with progressive neurocognitive decline and disordered white matter diffusion. In extreme cases, a diffuse necrotizing leukoencephalopathy can develop following intrathecal chemotherapy without or with radiotherapy. Rarely, patients with a remote history of intracranial irradiation present with headaches and neurological deficits and are found to have abnormal cortical enhancement. This entity has been termed stroke-like migraine attacks after radiation therapy (SMART) syndrome and is self-limited with resolution of imaging findings and symptoms the course of weeks.^[15] Additionally, with increased adoption of SWI in routine neuroimaging scattered foci of susceptibility are readily identified in the years following irradiation. While their pathogenesis is not fully understood, these small microhemorrhages or vascular malformations are thought to represent delayed radiation toxicity on cerebral microvasculature. Another late adverse effect of radiation therapy is the development of a second neoplasm. Radiation associated tumors, in decreasing order of frequency, include meningioma, gliomas, and sarcomas.^[16]

V. Conclusion

Brain tumor is a dreaded pathology which requires timely accurate diagnosis and initiation of suitable therapy. The past several decades have seen the widespread adoption of advanced MRI techniques in addition to conventional structural MRI for the routine clinical assessment of brain tumors. The incorporation of these biology-driven MRI methods has been indispensable to the neurosurgeon and contributed to improved diagnosis, surgical and radiosurgical planning, and assessment of treatment response. Imaging evaluation with magnetic resonance imaging (MRI) plays an important role in diagnosis and timely management of brain and spinal cord tumors and will continue to evolve to reflect our growing understanding of brain tumor molecular genetics and targeted therapy with the overarching goal of being the objective and quantitative arbiter of therapy response for patients with brain tumor.

CONFLICT OF INTEREST: There are no conflicts of interest.

SOURCE OF SUPPORT: Nil

References

- [1]. Ellingson BM, Bendszus M, Boxerman J et al. Consensus recommendations for a standardized Brain Tumor Imaging Protocol in clinical trials. *Neuro Oncol.* 2015;17(9):1188-1198
- [2]. Nag S, Manias JL, Stewart DJ. Pathology and new players in the pathogenesis of brain edema. *Acta Neuropathol.* 2009;118(2):197-217
- [3]. Raz E, Zagzag D, Saba L et al. Cyst with a mural nodule tumor of the brain. *Cancer Imaging.* 2012;12(1):237-244.
- [4]. Mabray MC, Barajas RF Jr, Cha S. Modern brain tumor imaging. *Brain Tumor Res Treat.* 2015;3(1):8-16.
- [5]. Xiao H-F, Chen Z-Y, Lou X et al. Astrocytic tumour grading: a comparative study of threedimensional pseudocontinuous arterial spin labelling, dynamic susceptibility contrast-enhanced perfusion-weighted imaging, and diffusion-weighted imaging. *Eur Radiol.* 2015;25(12):3423-3430.
- [6]. Radbruch A, Wiestler B, Kramp L et al. Differentiation of glioblastoma and primary CNS lymphomas using susceptibility weighted imaging. *Eur J Radiol.* 2013;82(3):552-556.

[7]. Essig M, Nguyen TB, Shiroishi MS et al. Perfusion MRI: the five most frequently asked clinical questions. Am J Roentgenol. 2013;201(3):W495-W510.

[8]. Jain R. Measurements of tumor vascular leakiness using DCE in brain tumors: clinical applications. NMR Biomed. 2013;26(8):1042-1049.

[9]. Qiao XJ, Ellingson BM, Kim HJ et al. Arterial spin-labeling perfusion MRI stratifies progression-free survival and correlates with epidermal growth factor receptor status in glioblastoma. Am J Neuroradiol. 2015;36(4):672-677

[10]. Bulik M, Jancalek R, Vanicek J, Skoch A, Mechl M. Potential of MR spectroscopy for assessment of glioma grading. Clin Neuro Neurosurg. 2013;115(2):146-153.

[11]. Mandelli ML, Berger MS, Bucci M, Berman JI, Amirbekian B, Henry RG. Quantifying accuracy and precision of diffusion MR tractography of the corticospinal tract in brain tumors. J Neurosurg. 2014;121(2):349-358

[12]. Roder C, Charyasz-Leks E, Breitung M et al. Resting-state functional MRI in an intraoperative MRI setting: proof of feasibility and correlation to clinical outcome of patients. J Neurosurg. 2016;125(2):401-409

[13]. Al-Okaili RN, Krejza J, Wang S, Woo JH, Melhem ER. Advanced MR imaging techniques in the diagnosis of intraaxial brain tumors in adults. Radiographics. 2006; 26 (suppl 1):S173-S189

[14]. Lotumolo A, Caivano R, Rabasco P et al. Comparison between magnetic resonance spectroscopy and diffusion weighted imaging in the evaluation of gliomas response after treatment. Eur J Radiol. 2015;84(12):2597-2604.

[15]. Nowosielski M, Wiestler B, Goebel G et al. Progression types after antiangiogenic therapy are related to outcome in recurrent glioblastoma. Neurology. 2014;82(19):1684-1692.

[16]. Hutterer M, Hattingen E, Palm C, Proescholdt MA, Hau P. Current standards and new concepts in MRI and PET response assessment of antiangiogenic therapies in high-grade glioma patients. Neuro Oncol. 2015;17(6):784-800.

CHART-1

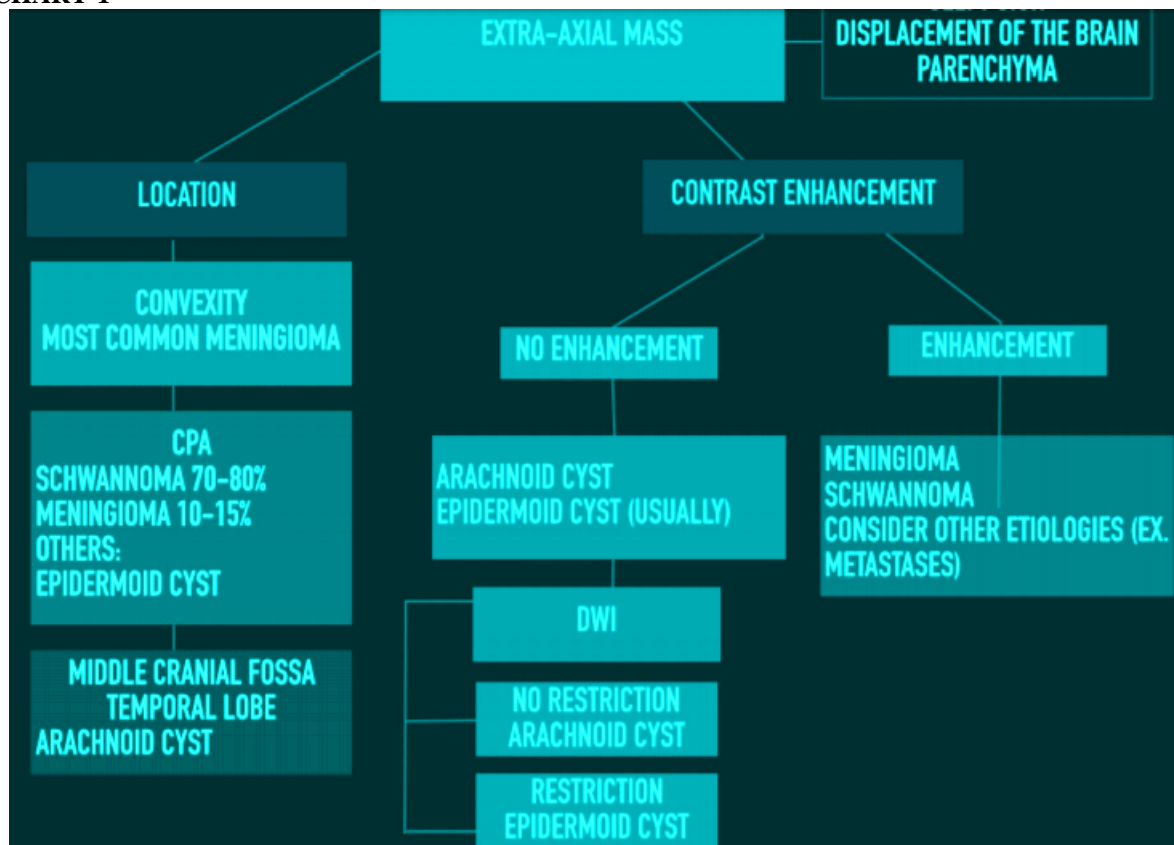


CHART-1: Algorithm for unknown extraaxial mass classification

CHART-2

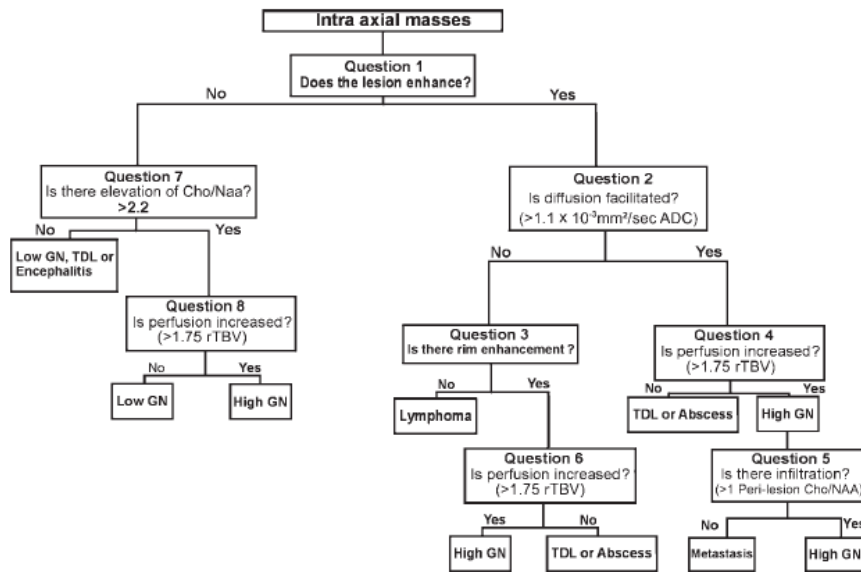


CHART-2: Algorithm for unknown intraaxial mass classification.

Cho - choline, High GN- high-grade neoplasm, Low GN - low-grade neoplasm, TDL-tumefactive demyelinating lesion.

CHART-3

Typical Advanced MR Imaging Features of Intraaxial Brain Tumors

MR Imaging Feature	Neoplasms			Tumefactive Demyelinating Lesion	Abscess*	Encephalitis
	Primary	Secondary	Lymphoma			
MR spectroscopy						
Lipid signal (ppm)	Elevated at 0.9 and 1.3, especially with high-grade lesion	Elevated at 0.9 and 1.3	Elevated at 0.9 and 1.3
Lactate signal (ppm)	Elevated at 1.33, especially with high-grade lesion	Elevated at 1.33	Elevated at 1.33	...	Elevated at 1.33	Elevated at 1.33
NAA signal (ppm)	Reduced at 2.02, more so with high-grade lesion	Reduced or absent at 2.02	Reduced at 2.02	Reduced at 2.02	Absent at 2.02	Reduced at 2.02
Choline signal (ppm)	Elevated at 3.2, more so with high-grade lesion	Elevated at 3.2	Elevated at 3.2	Elevated at 3.2, especially with acute lesions	Absent at 3.2	Elevated at 3.2
Myoinositol signal (ppm)	Elevated at 3.55, more so with gliomatosis and low-grade lesion	Elevated at 3.55
Diffusion-weighted imaging: ADC value	Variable, 0.82-2.73 x 10 ⁻³ mm ² /sec	Elevated	Reduced	Reduced (crescent or concentric areas) for acute lesions; elevated for chronic lesions	Markedly reduced	Variable
Perfusion imaging: rTBV value	Tends to increase with tumor grade	Elevated	Low, compared with primary high-grade neoplasms; high, relative to toxoplasmosis	Low	Low	Unknown

*Other typical MR spectroscopic features include elevated signals for amino acid (at 0.9 ppm), alanine (at 1.47 ppm), acetate (at 1.92 ppm), pyruvate (at 2.37 ppm), and succinate (at 2.40 ppm), and absent creatine signal (at 3.0 ppm).

Chart 3: Typical Advanced MR Imaging Features of Intraaxial Brain Tumors

Chart 4: Types of brain tumors in adult age group

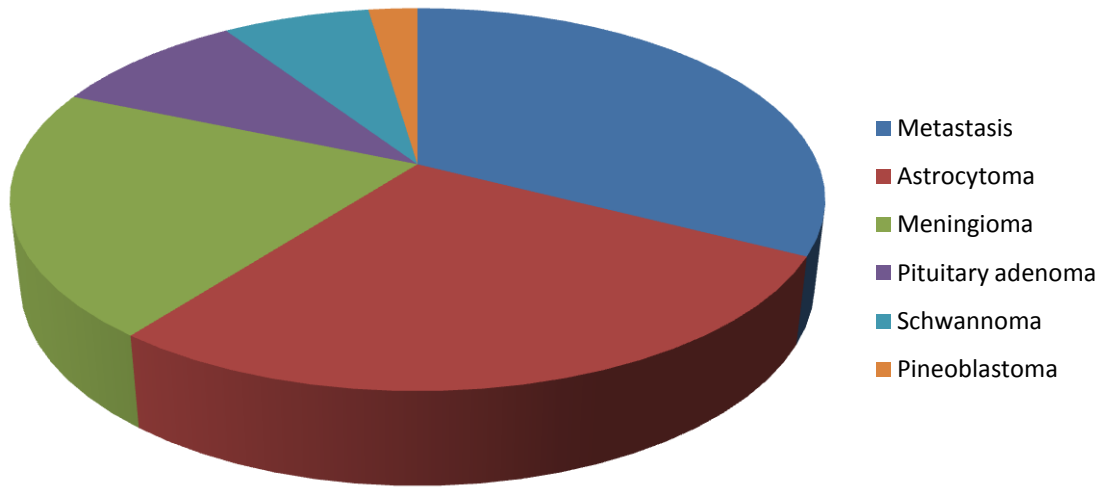


Chart 5: Types of Brain tumors in pediatric age group

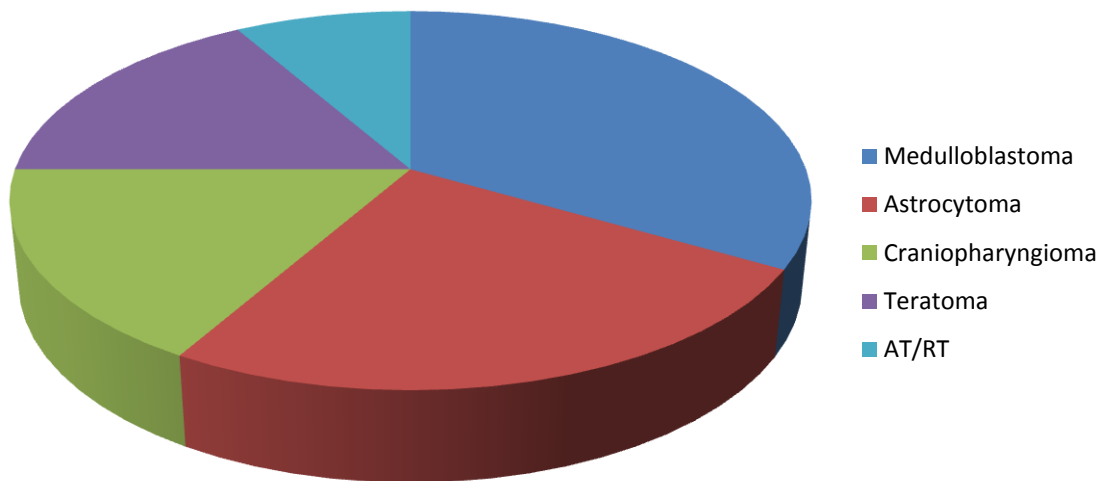


Chart 6: Types of Astrocytoma in Adult patients

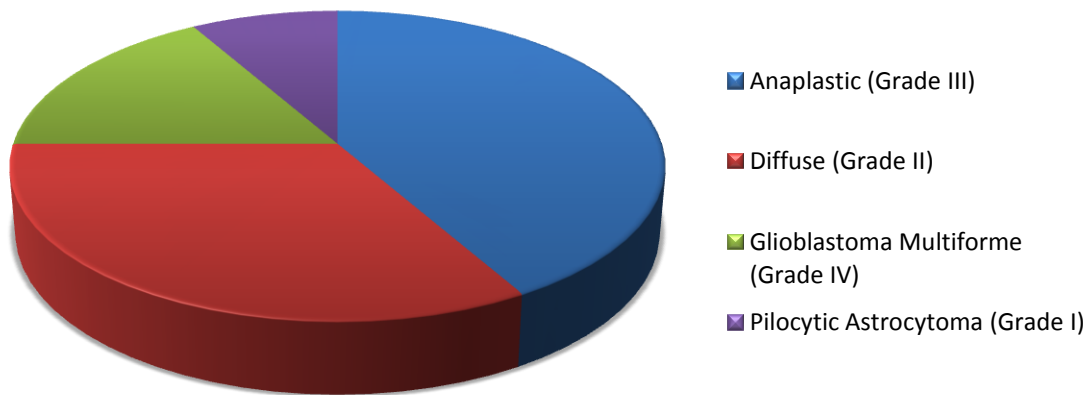


Chart 7: Source of primaries in our patients of Brain Metastasis

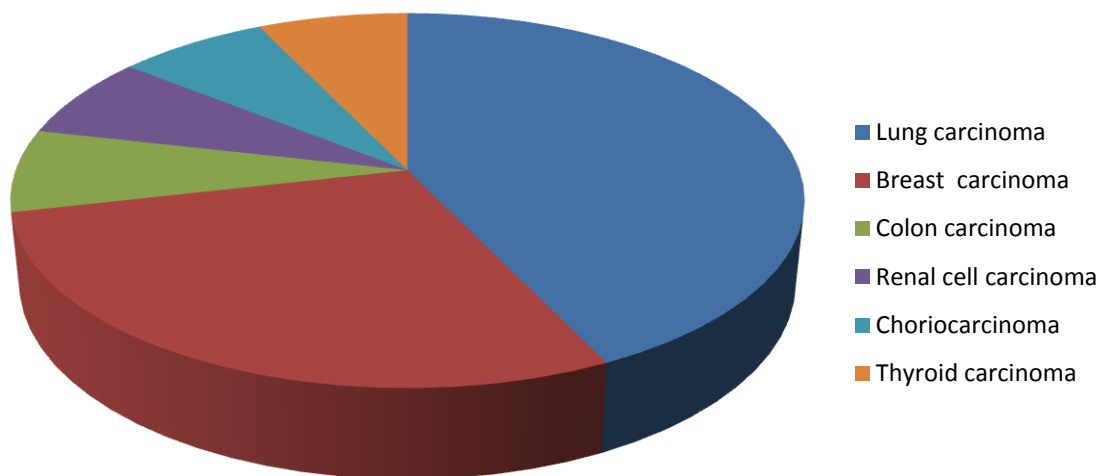


Chart 8: Sex distribution of overall patients of brain & spinal cord tumors in our study

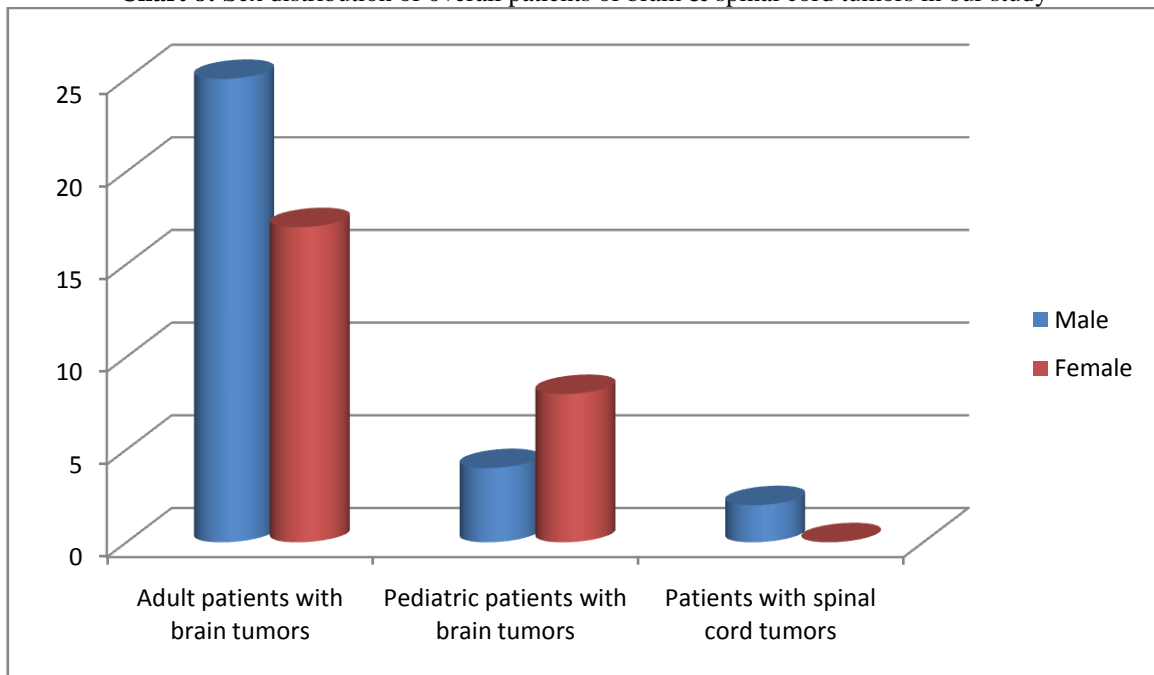
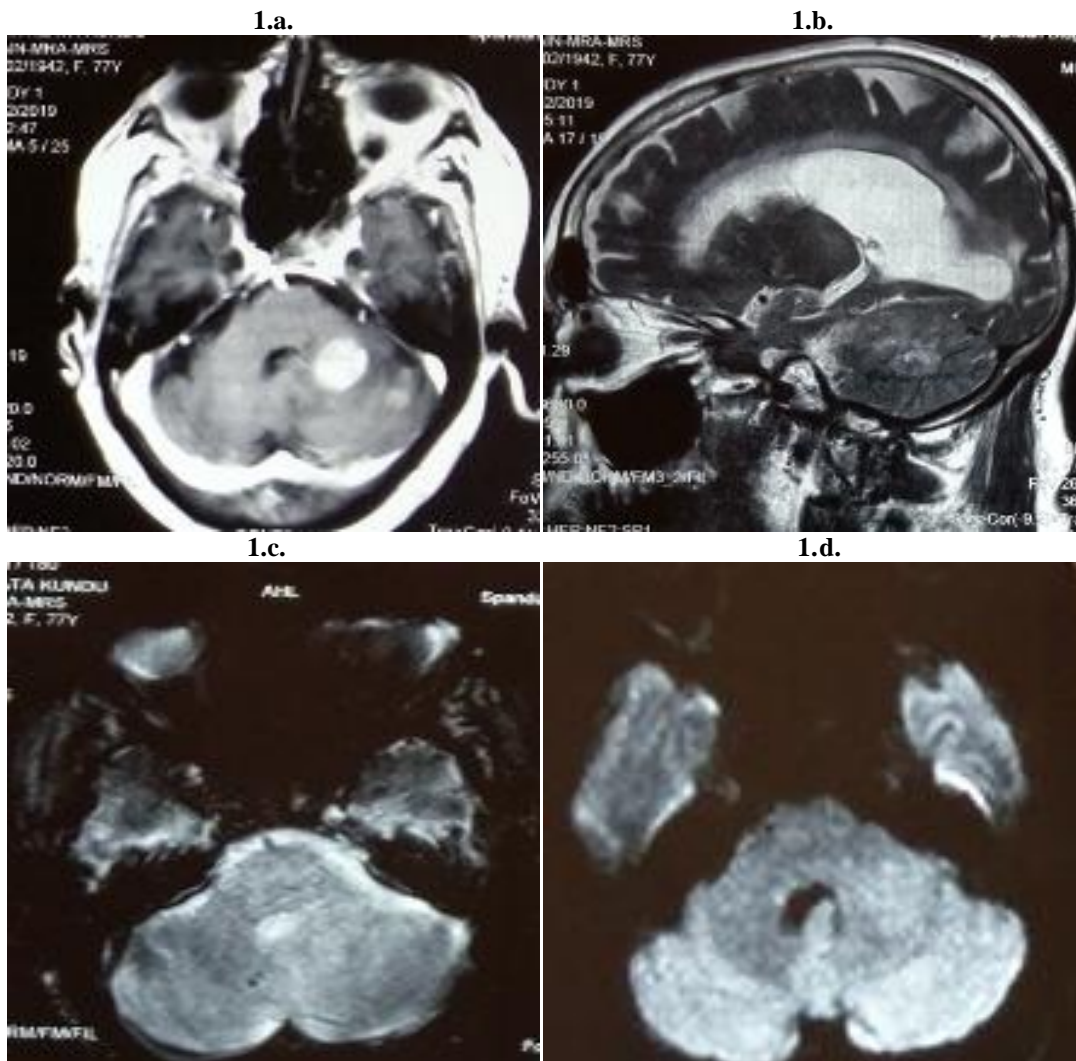


FIGURE 1:



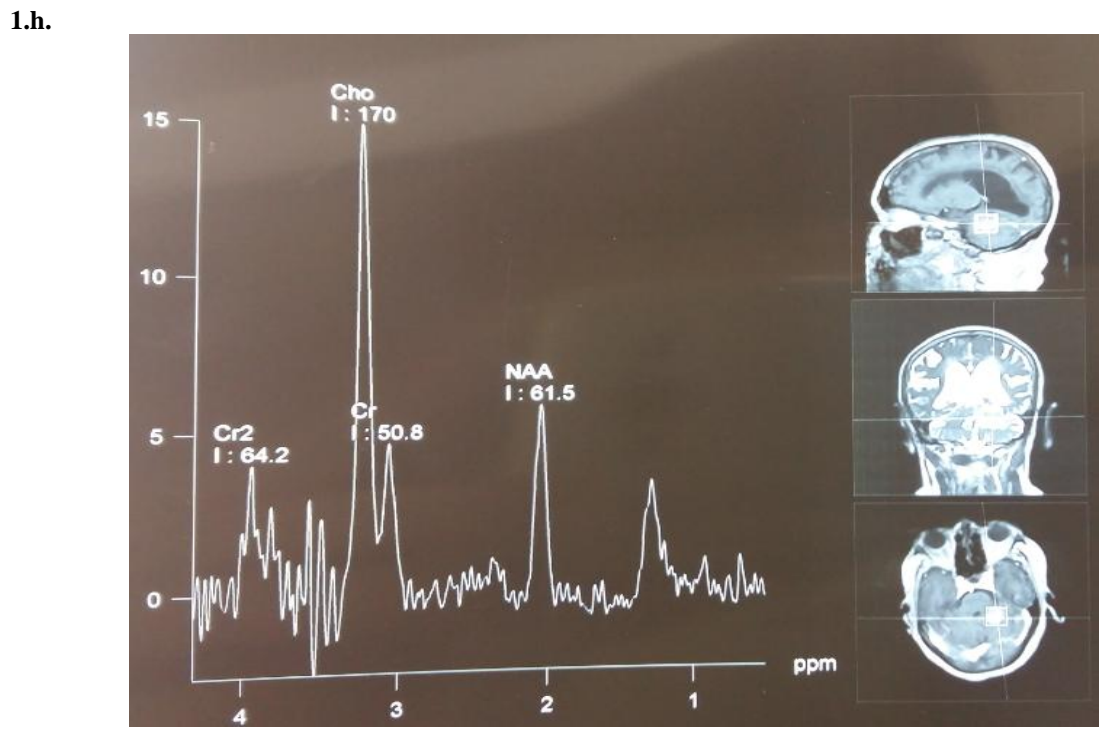
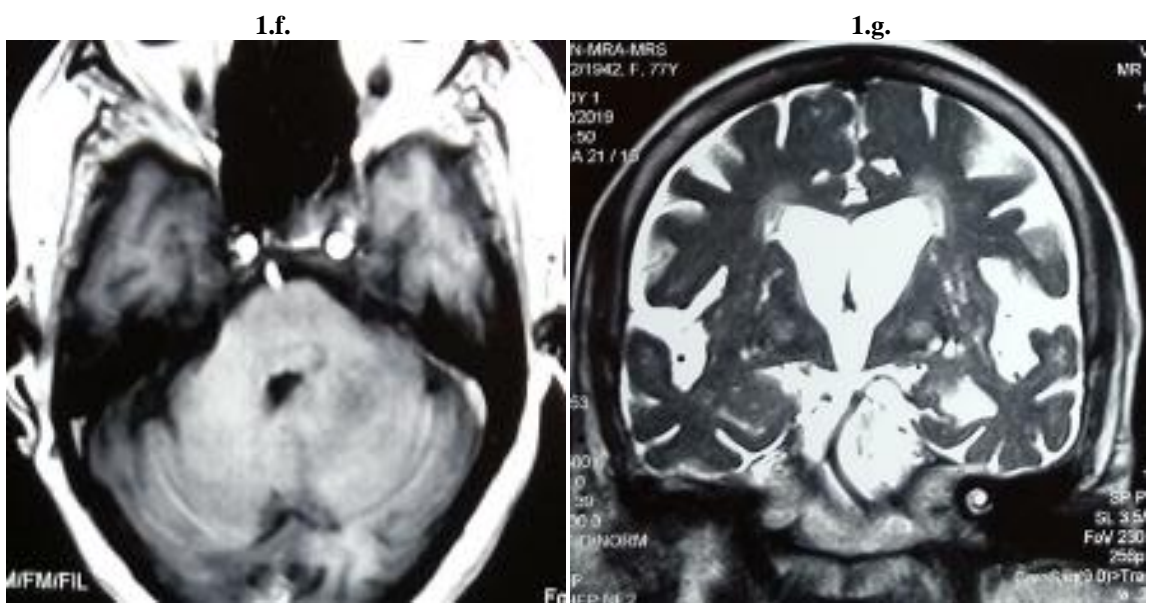
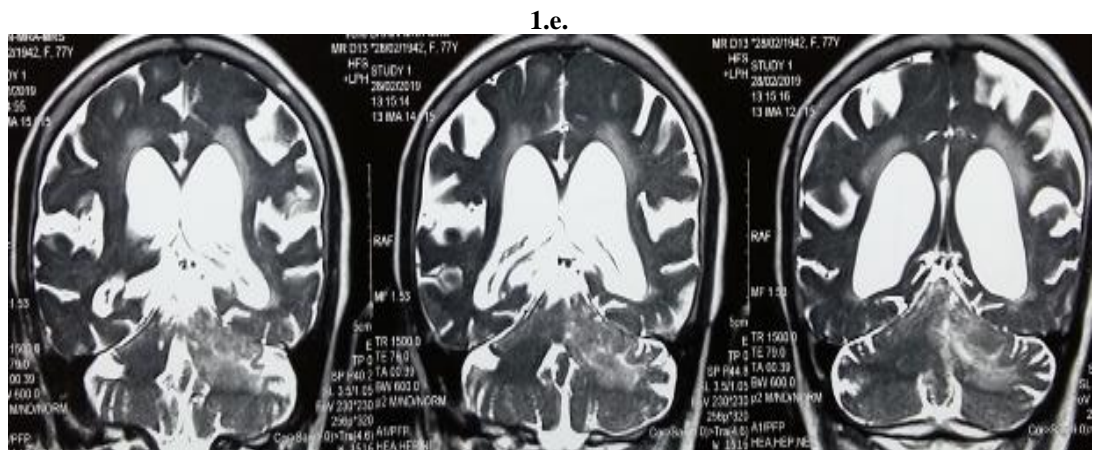
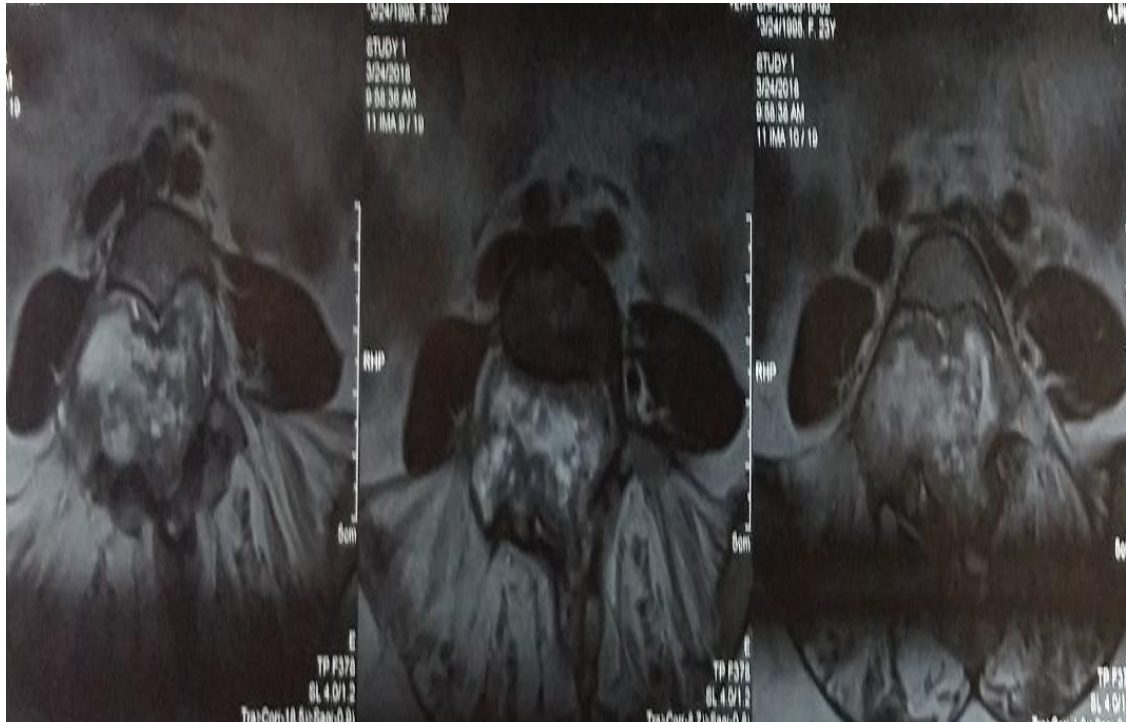


Figure 1: MR images show a SOL in the left cerebellum near the 4th ventricle in a 57 year old male presenting with ataxia and stroke like features. The tumor is iso to hypointense in T1W images (1.f.), heterogeneously hyperintense in T2W imaging (1.b, 1.e, 1.g.), does not suppress in T2-FLAIR (1.a.), shows no significant diffusion restriction in DWI and ADC maps (1.c, 1.d.) and shows high levels of Choline and low levels of NAA in MR Spectroscopy images, revealing its neoplastic nature. Histopathology revealed Diffuse astrocytoma (Grade 2).

FIGURE-2:

2.a.



2.b.



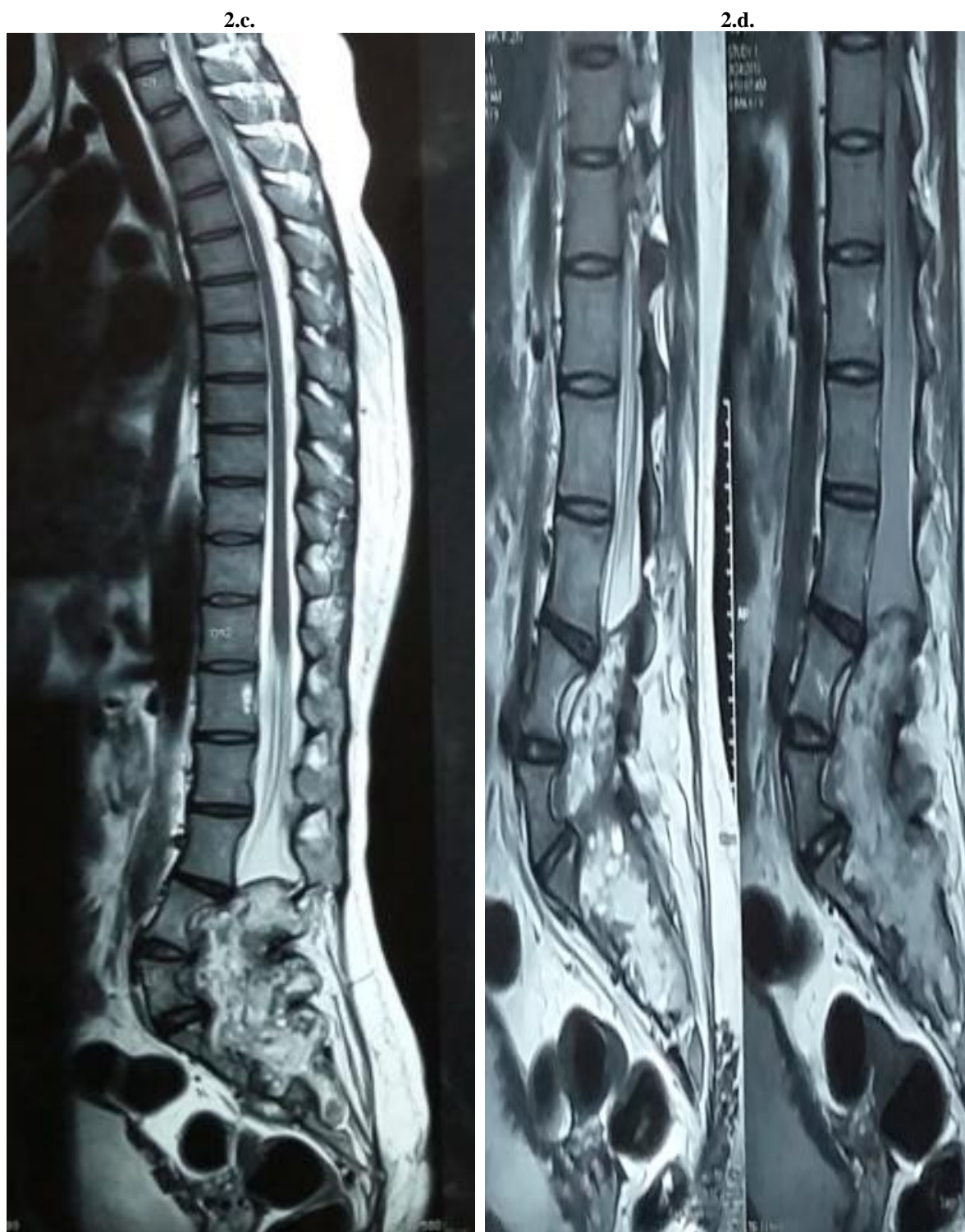
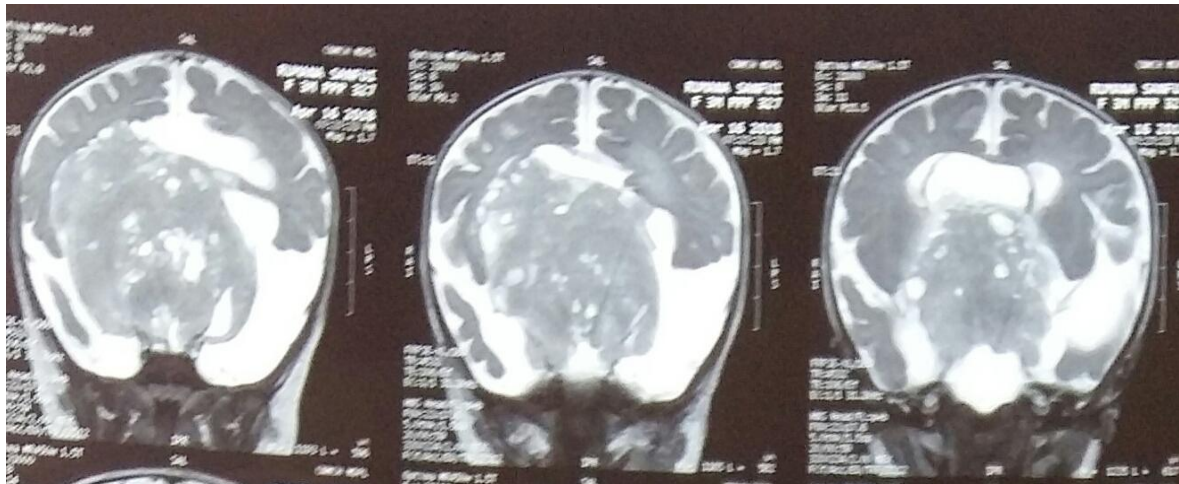


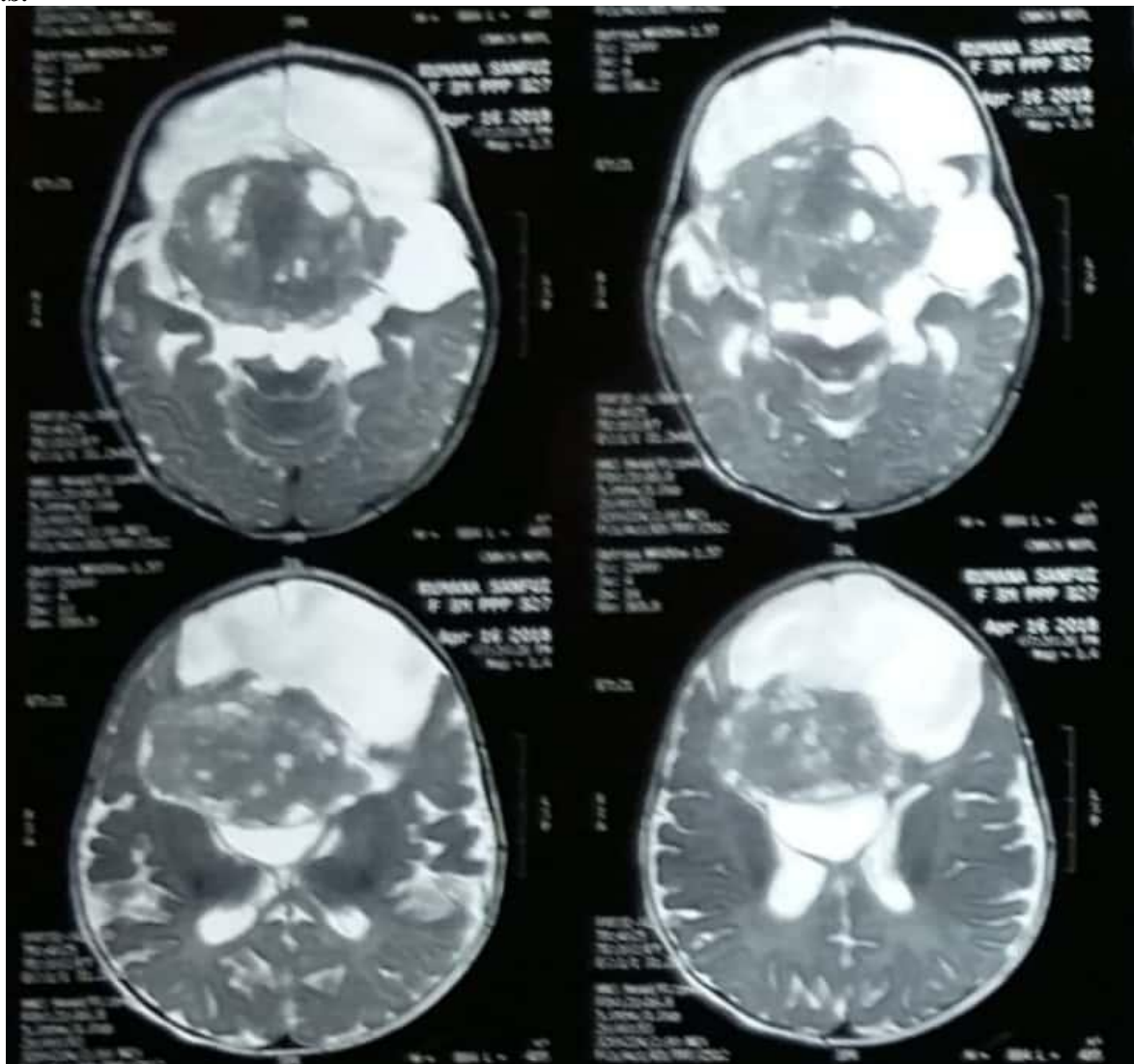
Figure 2: The patient was a 33 year old female presenting with back pain and neurogenic bladder. MRI revealed well defined vividly enhancing T1 iso and T2 heterogenous hyperintense lesion within the intradural region of spinal canal extending from L4 to S3 level causing widening of the canal with scalloping of posterior aspect of adjacent vertebral bodies and erosion of the bilateral pedicles, laminae of L4 and L5 and spinous process of L5 with extension along exiting nerve roots through lumbar and sacral neural foramina. Diagnosis of Neurofibroma was made, which was corroborated by Histopathological examination.

FIGURE-3:

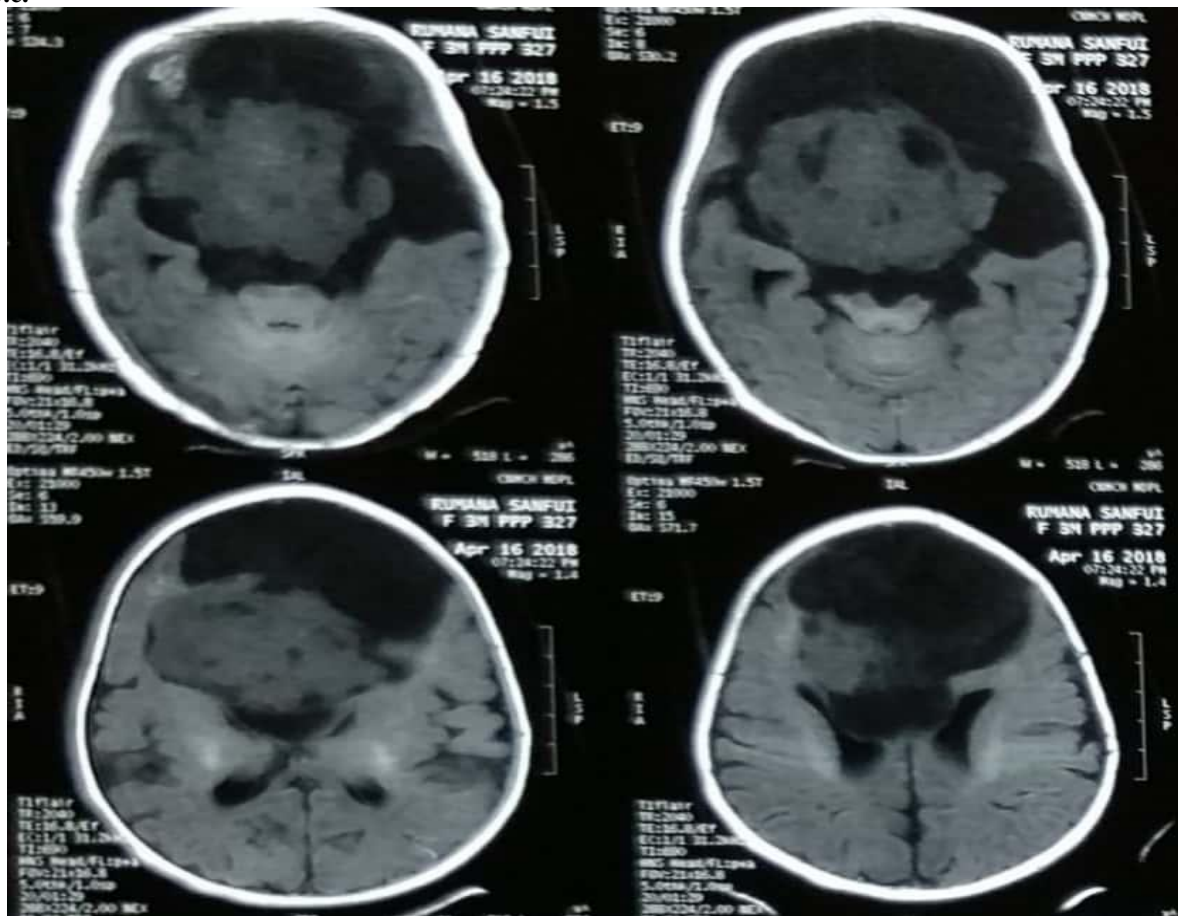
3.a.



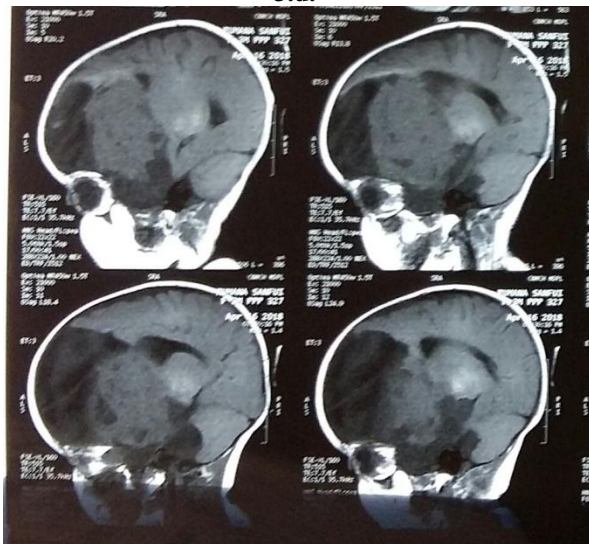
3.b.



3.c.



3.d.



3.e.

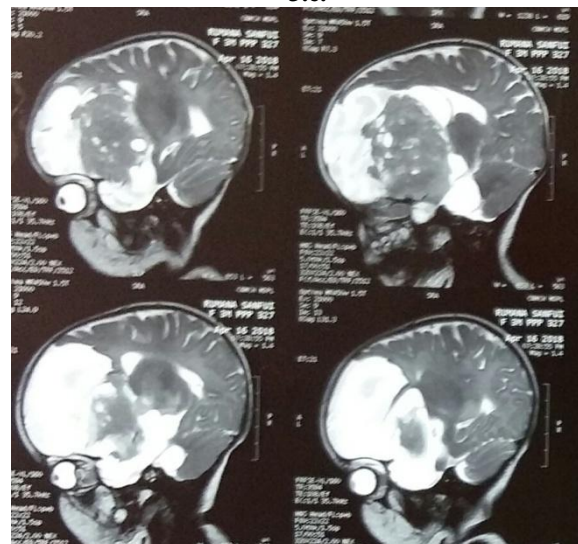


Figure 3: Midline large tumor involving anterior and middle cranial fossa in a 1.5 year old male child presenting with progressively worsening sensorium, headache and vomiting of 1 month duration. The mass is iso to hyperintense on T1W MR image (3.c, 3.d) and heterogeneously hyperintense on T2W MR image (3.a,3.b,3.e.) compared with surrounding normal brain tissue. There are multiple cystic areas, hemorrhage and necrosis in the SOL. Histopathological examination revealed Grade IV Atypical Rhabdoid/Teratoid Tumor (AT/RT).

FIGURE-4:

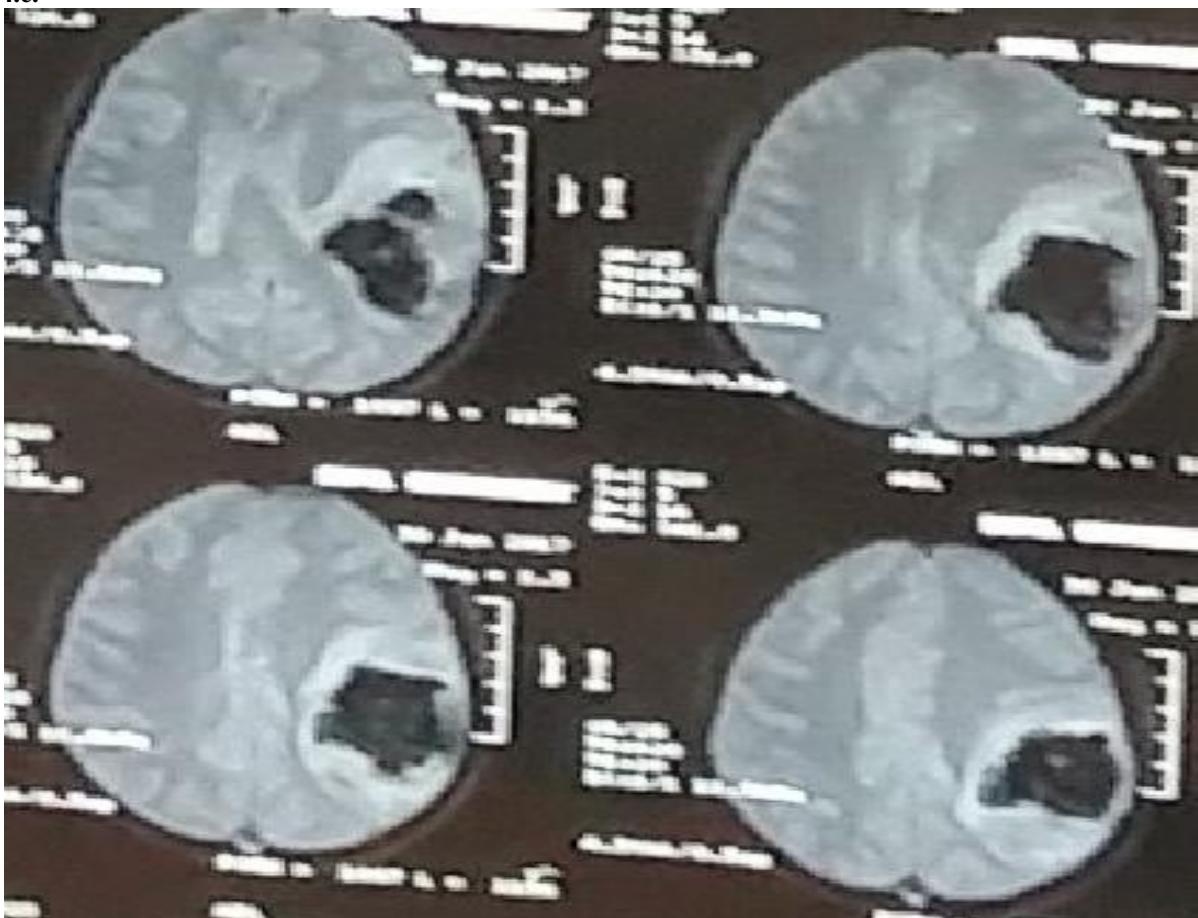
4.a.



4.b.



4.c.



4.d.



4.e.



Figure 4: The patient was a 65 years old male, presenting with paraparesis of lower limbs and right upper limb, gradually increasing dull headache and worsening sensorium over 3 weeks. There was no history of trauma. MRI brain revealed a large intraaxial mass of heterogeneous intensity in both T1W (4.b.) and T2W (4.a.) imaging with extensive areas of hemorrhage, necrosis and surrounding edema. Evidence of large area of hemorrhage and necrosis was also there in GRE (4.c.) and SW (4.d.) images. MRI of spine (4.e.) revealed a drop metastasis in lumbar region. Histopathological examination confirmed Grade IV Glioblastoma Multiforme with drop metastasis to spinal cord.

Dr. Nupur Basu, Dr. Prithvijit Chakraborty. “Radiological Evaluation of Spectrum of Neurooncological Pathologies: Our Experience in a Tertiary Care Hospital of Eastern India”. IOSR Journal of Dental and Medical Sciences (IOSR-JDMS), vol. 18, no. 04, 2019, pp 46-62.